Investigation of Volume Changes in Carbon Dioxide Hydrate Formation Process

A. Mohammadi[1*], M. Hakimizadeh[2]

[1] Department of Chemical Engineering, University of Bojnourd, Bojnord, Iran
[2] Department of Chemical Engineering, Babol Noshirvani University of Technology, Babol, Iran

A B S T R A C T

Gas hydrate formation is a new technology to uptake carbon dioxide. In the present work, the kinetics of changes in the volume of unreacted water, the formed carbon dioxide hydrate, and also the unreacted gas inside the reactor were investigated with the passage of time. Experiments were performed in a stagnant 169 cm^3 double-walled reactor at a temperature of 275.15 K and a pressure of 3 MPa. The tests were done by using the isochoric-isothermal method. The results of the experiments showed that the volume of unreacted water decreased with respect to time and the volume of hydrate formed increased. Taking into account the different molar volumes of hydrate formed and the molar volume of reacted water in the test conditions, the changes in gas volume inside the reactor were calculated with the passage of time. The gas volume inside the reactor decreased from 144 cm^3 at the beginning of the process to 141.62 cm^3 at the end of the reaction. By decreasing the pressure during carbon dioxide hydrate formation process, the amount of hydration number increased from 6.047 mol/mol to 6.109 mol/mol.

doi: 10.5829/ijee.2024.15.02.02

NOMENCLATURE

M	Hydration number		S	Small
V_{s0}	Initial volume of feed solution (m^3)		C	Langmuir constant
V_{cell}	Cell volume (m^3)		V	Volume (m^3)
f	Fugacity (Pa)		θ	Fractional occupancy
Subscripts			Δn	Gas mole change (mole)
RW	Reacted water		v_w^L	Molar volume of water (m^3/mole)
L	Large			

INTRODUCTION

Global activities are contributing to a continuous increase in human carbon dioxide emissions, resulting in elevated levels of this gas in the atmosphere. Since 1958, the level of carbon dioxide in the atmosphere has risen by 22%, and since 1880, it has increased by 30%. This alarming rise in carbon dioxide levels has had significant impacts on the climate. For instance, global temperature measurements indicate an increase in the average annual surface temperature of 0.3 to 0.6°C over the past 159 years [1]. If this upward trend in temperatures continues, the detrimental effects of global warming on the world's population will become unavoidable. Consequently, concerns about the escalating levels of carbon dioxide and other greenhouse gases in the atmosphere have prompted global apprehension, leading to international initiatives such as the Kyoto Protocol and the Paris Agreement. The

Corresponding Author Email: mohammadi.a@ub.ac.ir
(A. Mohammadi)

primary sources of carbon dioxide emissions in the atmosphere include thermal power generation, oil and natural gas refining and processing, cement production, the iron and steel industries, and petrochemical industries [2]. Therefore, it is crucial to remove this gas from the emissions of industrial complexes to mitigate the negative impacts of climate change. The hydrate formation process is among the latest methods used for carbon dioxide absorption. Gas hydrates are crystal structures resembling ice, which form when they encounter low-density gases like methane, ethane, or carbon dioxide at low temperatures and high pressures [3–8]. Figure 1 illustrates the hydrogen bonding between water molecules.

In recent years, the potential benefits of gas hydrates have garnered attention, leading to numerous studies in the field [9–21]. However, due to the high costs and time-consuming nature of the hydrate formation process, none of the proposed processes utilizing hydrate formation have been implemented on an industrial scale [22–27]. Figure 2 presents a real image of methane hydrate formed in a laboratory reactor.

SI, SII, and SH are three prevalent structures of gas hydrates. These structures exhibit distinct shapes, including variations in the types and numbers of cavities they possess. The SI structure, also known as structure I, is the most common type of gas hydrate. It consists of cages formed by interc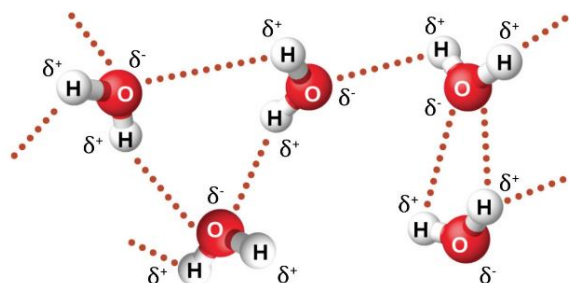onnected water molecules, which enclose the guest gas molecules. These cages can be further classified into large, small, and intermediate sizes, depending on the number of water molecules they comprise. The SII structure, or structure II, is characterized by a more complex arrangement. It contains two types of cages: large and small. The large cages are similar to those in the SI structure, while the small cages are formed by linking water molecules through face-sharing. The SH structure, or structure H, is relatively less common but still significant. It consists of hexagonal-shaped cages, unlike the cubic cages found in SI and SII structures. These hexagonal cages offer a unique configuration for hosting gas molecules. Figure 3 provides a visual representation of these structures, highlighting their unique characteristics.

Due to the difference between the molar volume of the formed hydrate and the molar volume of the reacted water, the volume of gas inside the reactor changes by time in the process of gas hydrate formation. In this research, we calculate the volume of unreacted water and volume of hydrate formation versus the time and gas volume changes inside the reactor, in the process of carbon dioxide hydrate formation.

MATERIAL AND METHODS

Materials
To prepare the solutions, distilled water was used. Carbon dioxide, with a purity of 99.99 mol%, was supplied by Sepehr Kavian Gas company.

Apparatus
Figure 4 shows the schematic diagram illustrating the apparatus utilized in the current study. The used appartus
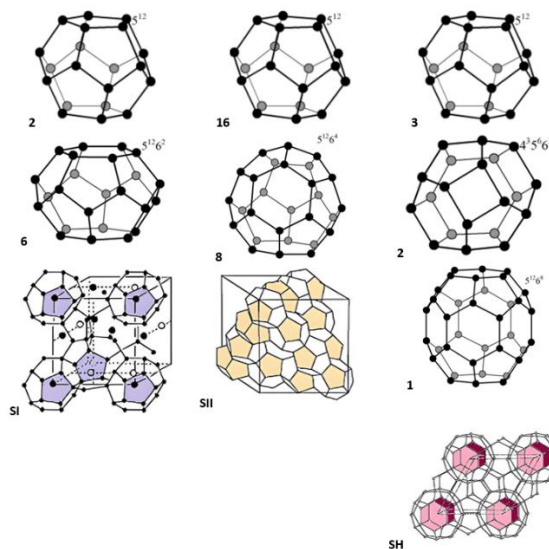

Figure 1. The hydrogen bonding between water molecules

Figure 2. A real image of methane hydrate formed in a laboratory reactor

Figure 3. The shape of the conventional structures of gas hydrates

Table 1. The characteristics of the conventional structures of gas hydrates [28]

Property	Hydrate						
	Structure I (SI)		Structure II (SII)		Structure H (SH)		
Caviaty type	Small 5^{12}	Large $5^{12}6^2$	Small 5^{12}	Large $5^{12}6^4$	Medium $4^35^66^3$	Small 5^{12}	Large $5^{12}6^8$
Radius (A)	3.95	4.33	3.91	4.73	4.06	3.91	5.71
Cages/ unit cell	2	6	16	8	2	3	1
H_2O Molecules/cell	46		136		34		
Crystal type	Cubic		Cubic		Hexagonal		
Guest molecules	Methane, Carbon dioxide		Propane, Nitrogen		Methane + Neohexane		

in this research is fully described in our previous research [10]. Th used apparaus is equipped with a thermometer (PT100) and a pressure transducer. The standard uncertainties, u, of measured temperature and pressure are u(T) = 0.1 K and u(P) = 5 kPa, respectively.

RESULTS AND DISCUSSION

To ensure the accuracy of the pressure and temperature tranducers, we measured the three-phase equilibrium data of carbon dioxide hydrate formation using an isochoric pressure-search method [29–33]. The measured equilibrium data in this work and the data reported by Vlahakis and coworkers [34] are depicted in Figure 5.

As can be seen in Figure 5, the measured data in this work are in a good agreement with the data reported by Vlahakis and coworkers [34] that confirm the accuracy of our pressure and temperature tranducers.

The measured equilibrium data of carbon dioxide hydrate formation are tabulated in Table 2.

In each kinetic experiment, the hydrate formation cell is initially rinsed with water, followed by a rinse with distilled water. The vacuum pump is employed to remove the air from the reactor, and subsequently, 25 cm^3 of solution is injected into the cell. Using a temperature bath, the reactor is set to a temperature of 275.15 K. The hydrate-forming gas, in this case carbon dioxide, is
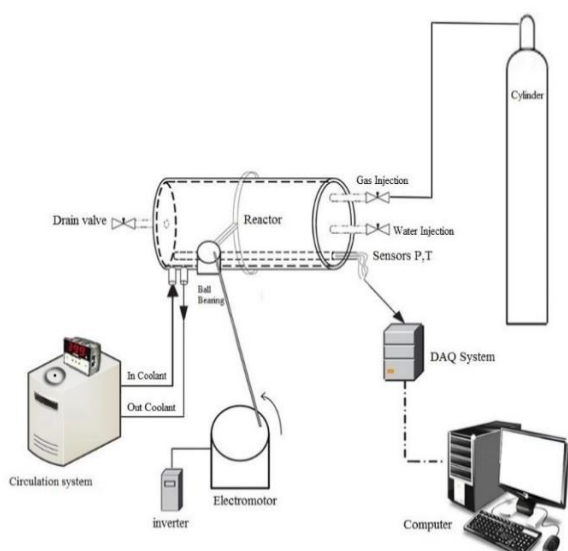

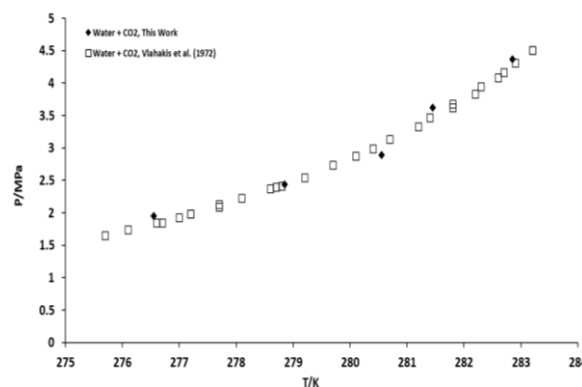**Figure 5.** The three-phase equilibrium data of carbon dioxide hydrate formation: ◆, this work; □, pure carbon dioxide


Figure 4. Schematic diagram of the experimental apparatus used for the kinetic studies

Table 2. The measured equilibrium data of carbon dioxide hydrate formation

T (K)	P (MPa)
276.55	1.95
278.85	2.44
280.55	2.89
281.45	3.62
282.85	4.37

introduced into the cell until the desired pressure is reached. It is important to position the reactor horizontally and refrain from using the stirrer method.

The equilibrium system required sufficient time, the process of hydrate formation commences, leading to a decrease in system pressure until it reaches a stable condition where pressure changes inside the reactor are minimal (0.05 h/bar). The quantity of gas consumed during the hydrate formation process is determined through calculations using Peng-Robinson equation of state [35]. Throughout the hydrate formation process, the computer records the temperature and pressure of the system at intervals of 20 seconds.

The physical reaction between water and gas molecules (for example, carbon dioxide to form hydrate can be shown as follows [36]:

$$CO_2 + MH_2O \longleftrightarrow CO_2 \bullet MH_2O \tag{1}$$
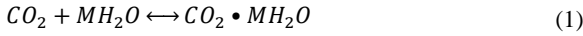
where M represents the hydration number. Simple gases methane and carbon dioxide form the sI hydrate structure in absence of thermodynamic additives. The hydration number is a parameter that depends on the filling of large and small cavities. The hydration number for structure sI can be calculated from the following equation [10]:

$$M = \frac{46}{6\theta_L + 2\theta_S} \tag{2}$$

In this relation, θ_L and θ_S are the occupancy fractional of large (L) and small (S) cavities, respectively, which are calculated using the Languire absorption theory as stated as follows [10].

$$\theta_i = \frac{C_i f_{CO_2}}{1 + C_i f_{CO_2}} \tag{3}$$

where C_i is the Langmuir constant of carbon dioxide molecules for type i cavities and f_{CO_2} is the fugacity of carbon dioxide in the gas phase, which is calculated using Peng-Robinson equation of state. The subscript i also represents the type i cavity.

As the solution and gas hydrate have different molar volumes, the volume of gas within the cell decreases during the formation and growth of the gas hydrate. Consequently, the instantaneous volume of gas inside the cell, denoted as V_t, can be determined using the following equation:

$$V_t = V_{cell} - V_{S_0} + V_{RW_t} - V_{H_t} \tag{4}$$

which are V_{cell} and V_{s0} are cell volume (169 cm^3) and initial volume of feed solution (25 cm^3), respectively. Also, V_{RW_t} and V_{H_t} represent the volume of reacted water and the volume of hydrate produced, respectively. The subscript t in the above equation indicates that these parameters are a function of time. The volume of reacted water is calculated from the following equation:

$$V_{RW_t} = M \times \Delta n_{CO_2} \times v_w^L \tag{5}$$

The amount of calculated hydration numbe during hydrate formation are shown in Figure 6.

As shown in Figure 6, as the hydrate formation process proceeds, the amount of hydration number increases. This can be due to the pressure reduction due to the carbon dioxide hydrate growth.

Figure 7 displays the temporal variations in volume for both the unreacted solution and the hydrate formed within the reactor. It is evident that as time progresses, the volume of unreacted water within the reactor diminishes, while the volume of the formed hydrate increases.

At the onset of the process, the volume of unreacted water inside the reactor measures 25 cm^3, which reduces to 15.8 cm^3 by the conclusion of the process. Additionally, the volume of the formed hydrate at the end of the process amounts to 11.57 cm^3.

Figure 8 illustrates the variations in the volume of unreacted carbon dioxide gas within the reactor over time. This figure demonstrates the implementation of an advanced algorithm, as introduced by Mohammadi et al. [36], to track the changes in gas volume within the reactor as time elapses. It is evident from the figure that the volume of unreacted gas inside the reactor steadily decreases with respect to time.
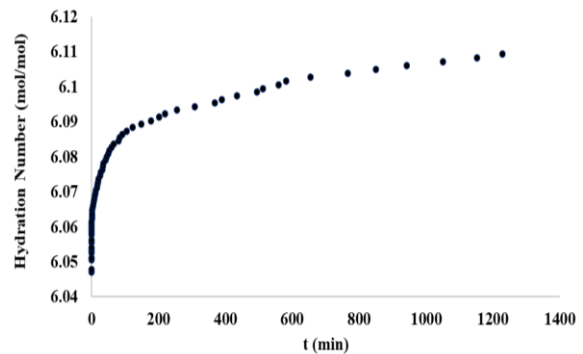

Figure 6. The amount of calculated hydration number during carbon dioxide hydrate formation process
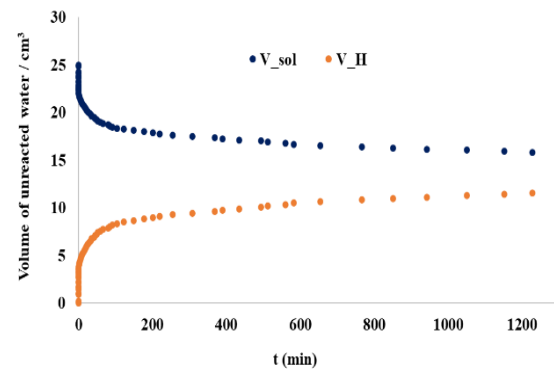

Figure 7. Changes in the volume of the unreacted solution as well as the hydrate formed inside the reactor
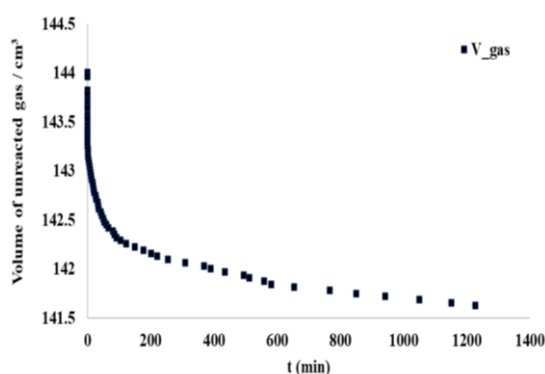
Figure 8. Changes in the volume of unreacted carbon dioxide inside the reactor

The observed phenomenon can be attributed to the disparity between the molar volume of the formed hydrate and the molar volume of the reacted water. As the molar volume of the formed hydrate exceeds that of water, the growth of the hydrate with respect to time leads to a reduction in the volume of the gaseous space within the reactor. Experimental results from a fixed horizontal reactor support this observation, revealing a decrease in gas volume from 144 cm^3 at the start of the process to 141.62 cm^3.

CONCLUSION

This study aimed to investigate the kinetics of volume changes in unreacted water, formed hydrate, and unreacted gas within the reactor with respect to time. Experimental results indicated a decrease in the volume of unreacted water and an increase in the volume of formed hydrate as time progressed. Considering the varying molar volumes of the formed hydrate and reacted water under the experimental conditions, changes in gas volume within the reactor were calculated with respect to time. The gas volume inside the reactor decreased from an initial value of 144 cm^3 to 141.62 cm^3 at the end of the reaction.

CONFLICT OF INTEREST

The authors declare that they have no known competing financial interests or personal relationships that could have appeared to influence the work reported in this paper.

REFERENCES

1. Nicholls, R.J., and Leatherman, S.P., 1996. Adapting to sea-level rise: Relative sea-level trends to 2100 for the United States. *Coastal Management*, 24(4), pp.301–324. Doi: 10.1080/08920759609362298

2. Pahlavanzadeh, H., Nouri, S., Mohammadi, A.H., and Manteghian, M., 2020. Experimental measurements and thermodynamic modeling of hydrate dissociation conditions in CO_2 + THF + NaCl + water systems. *The Journal of Chemical Thermodynamics*, 141, pp.105956. Doi: 10.1016/j.jct.2019.105956

3. Carroll, J., 2020. Natural Gas Hydrates: A Guide for Engineers. Gulf Professional Publishing.

4. Kim, E., Lee, S., Lee, J.D., and Seo, Y., 2015. Influences of large molecular alcohols on gas hydrates and their potential role in gas storage and CO_2 sequestration. *Chemical Engineering Journal*, 267, pp.117–123. Doi: 10.1016/j.cej.2015.01.023

5. Lee, Y., Lee, S., Lee, J., and Seo, Y., 2014. Structure identification and dissociation enthalpy measurements of the CO2+ N2 hydrates for their application to CO_2 capture and storage. *Chemical Engineering Journal*, 246, pp.20–26. Doi: 10.1016/j.cej.2014.02.045

6. Sloan, E.D., 2011. Natural Gas Hydrates in Flow Assurance. Gulf Professional Publishing.

7. Sloan, E.D., and Koh, C.A., 2007. Clathrate Hydrates of Natural Gases. CRC press.

8. Nguyen, N.N., Galib, M., and Nguyen, A. V., 2020. Critical Review on Gas Hydrate Formation at Solid Surfaces and in Confined Spaces—Why and How Does Interfacial Regime Matter? *Energy & Fuels*, 34(6), pp.6751–6760. Doi: 10.1021/acs.energyfuels.0c01291

9. Mohammadi, A., 2020. The roles TBAF and SDS on the kinetics of methane hydrate formation as a cold storage material. *Journal of Molecular Liquids*, 309, pp.113175. Doi: 10.1016/j.molliq.2020.113175

10. Mohammadi, A., Babakhanpour, N., Mohammad Javidani, A., and Ahmadi, G., 2021. Corn's dextrin, a novel environmentally friendly promoter of methane hydrate formation. *Journal of Molecular Liquids*, 336, pp.116855. Doi: 10.1016/j.molliq.2021.116855

11. Mohammadi, A., Fazli, R.H., and Asil, A.G., 2021. Influence of Tetra n-Butylammonium Chloride and Polysorbate 80 on the Kinetics of Methane Hydrate Formation. *Journal of the Japan Petroleum Institute*, 64(1), pp.22–28. Doi: 10.1627/jpi.64.22

12. Mohammadi, A., Kamran-Pirzaman, A., and Rahmati, N., 2021. The effect tetra butyl ammonium hydroxide and tween on the kinetics of carbon dioxide hydrate formation. *Petroleum Science and Technology*, pp.1–19. Doi: 10.1080/10916466.2021.1947321

13. Dong, H., Wang, J., Xie, Z., Wang, B., Zhang, L., and Shi, Q., 2021. Potential applications based on the formation and dissociation of gas hydrates. *Renewable and Sustainable Energy Reviews*, 143, pp.110928. Doi: 10.1016/j.rser.2021.110928

14. Wu, Q., Yu, Y., Zhang, B., Gao, X., and Zhang, Q., 2019. Effect of temperature on safety and stability of gas hydrate during coal mine gas storage and transportation. *Safety Science*, 118, pp.264–272. Doi: 10.1016/j.ssci.2019.04.034

15. Gambelli, A.M., Castellani, B., Nicolini, A., and Rossi, F., 2019. Gas hydrate formation as a strategy for CH_4/CO_2 separation: Experimental study on gaseous mixtures produced via Sabatier reaction. *Journal of Natural Gas Science and Engineering*, 71, pp.102985. Doi: 10.1016/j.jngse.2019.102985

16. Sergeeva, M.S., Mokhnachev, N.A., Shablykin, D.N., Vorotyntsev, A. V., Zarubin, D.M., Atlaskin, A.A., Trubyanov, M.M., Vorotyntsev, I. V., Vorotyntsev, V.M., and Petukhov, A.N., 2021. Xenon recovery from natural gas by hybrid method based on gas hydrate crystallisation and membrane gas separation. *Journal of Natural Gas Science and Engineering*, 86, pp.103740. Doi: 10.1016/j.jngse.2020.103740

17. Zheng, J., and Yang, M., 2020. Experimental investigation on

novel desalination system via gas hydrate. *Desalination*, 478, pp.114284. Doi: 10.1016/j.desal.2019.114284

18. Khan, M.N., Peters, C.J., and Koh, C.A., 2019. Desalination using gas hydrates: The role of crystal nucleation, growth and separation. *Desalination*, 468, pp.114049. Doi: 10.1016/j.desal.2019.06.015

19. Khan, M.S., Lal, B., Sabil, K.M., and Ahmed, I., 2019. Desalination of seawater through gas hydrate process: an overview. *Journal of Advanced Research in Fluid Mechanics and Thermal Sciences*, 55(1), pp.65–73

20. Mohammadi, A., 2022. The Effect of Various Concentrations of Tetra-n-butylammonium Fluoride on the Dissociation Enthalpy of Gas Hydrates. *Iranian Journal of Energy and Environment*, 13(2), pp.151–157. Doi: 10.5829/IJEE.2022.13.02.06

21. Montazeri, V., ZareNezhad, B., and Ghazi, A., 2022. Sequestration and Storage of Carbon Dioxide Using Hydrate Formation Method in the Presence of Copper Oxide Nanoparticles. *Iranian Journal of Energy and Environment*, 13(1), pp.46–54. Doi: 10.5829/IJEE.2022.13.01.06

22. Zhong, D.-L., Wang, Y.-R., Lu, Y.-Y., Wang, W.-C., and Wang, J.-L., 2016. Phase equilibrium and kinetics of gas hydrates formed from CO_2/H_2 in the presence of tetrahydrofuran and cyclohexane. *Journal of Natural Gas Science and Engineering*, 35, pp.1566–1572. Doi: 10.1016/j.jngse.2016.03.036

23. Chaturvedi, E., Laik, S., and Mandal, A., 2021. A comprehensive review of the effect of different kinetic promoters on methane hydrate formation. *Chinese Journal of Chemical Engineering*, 32, pp.1–16. Doi: 10.1016/j.cjche.2020.09.027

24. Yang, L., Wang, X., Liu, D., Cui, G., Dou, B., Wang, J., and Hao, S., 2020. Accelerated methane storage in clathrate hydrates using surfactant-stabilized suspension with graphite nanoparticles. *Chinese Journal of Chemical Engineering*, 28(4), pp.1112–1119. Doi: 10.1016/j.cjche.2019.12.009

25. Veluswamy, H.P., Bhattacharjee, G., Liao, J., and Linga, P., 2020. Macroscopic Kinetic Investigations on Mixed Natural Gas Hydrate Formation for Gas Storage Application. *Energy & Fuels*, 34(12), pp.15257–15269. Doi: 10.1021/acs.energyfuels.0c01862

26. Song, R., Yan, Y., Shang, L., Li, P., and Xu, J., 2020. A comparison of kinetics and thermodynamics of methane hydrate formation; dissociation in surfactant and solid dispersed emulsion. *Colloids and Surfaces A: Physicochemical and Engineering Aspects*, 599, pp.124935. Doi: 10.1016/j.colsurfa.2020.124935

27. Mahmood, M.E., and Al-Koofee, D.A.F., 2013. Effect of temperature changes on critical micelle concentration for tween

series surfactant. *Global Journal of Science Frontier Research Chemistry*, 13(1), pp.1–8

28. Sun, Q., and Kang, Y.T., 2016. Review on CO2 hydrate formation/dissociation and its cold energy application. *Renewable and Sustainable Energy Reviews*, 62, pp.478–494. Doi: 10.1016/j.rser.2016.04.062

29. Mohammadi, A., Manteghian, M., and Mohammadi, A.H., 2013. Dissociation Data of Semiclathrate Hydrates for the Systems of Tetra- n -butylammonium Fluoride (TBAF) + Methane + Water, TBAF + Carbon Dioxide + Water, and TBAF + Nitrogen + Water. *Journal of Chemical & Engineering Data*, 58(12), pp.3545–3550. Doi: 10.1021/je4008519

30. Bardool, R., Javanmardi, J., Roosta, A., and Mohammadi, A.H., 2016. Phase stability conditions of clathrate hydrates for methane+aqueous solution of water soluble organic promoter system: Modeling using a thermodynamic framework. *Journal of Molecular Liquids*, 224, pp.1117–1123. Doi: 10.1016/j.molliq.2016.09.084

31. Belandria, V., Mohammadi, A.H., Eslamimanesh, A., Richon, D., Sánchez-Mora, M.F., and Galicia-Luna, L.A., 2012. Phase equilibrium measurements for semi-clathrate hydrates of the (CO_2+N_2+tetra-n-butylammonium bromide) aqueous solution systems: Part 2. *Fluid Phase Equilibria*, 322–323, pp.105–112. Doi: 10.1016/j.fluid.2012.02.020

32. Lee, S., Lee, Y., Park, S., and Seo, Y., 2010. Phase Equilibria of Semiclathrate Hydrate for Nitrogen in the Presence of Tetra- n -butylammonium Bromide and Fluoride. *Journal of Chemical & Engineering Data*, 55(12), pp.5883–5886. Doi: 10.1021/je100886b

33. Lin, W., Delahaye, A., and Fournaison, L., 2008. Phase equilibrium and dissociation enthalpy for semi-clathrate hydrate of CO2+TBAB. *Fluid Phase Equilibria*, 264(1–2), pp.220–227. Doi: 10.1016/j.fluid.2007.11.020

34. Vlahakis, J.J., 1972. The Growth Rate of Ice Crystals: The Properties of carbon dioxide hydrate a review of properties of 51 gas hydrates. *Office of Water*, 830, pp.56–86

35. Peng, D.-Y., and Robinson, D.B., 1976. A New Two-Constant Equation of State. *Industrial & Engineering Chemistry Fundamentals*, 15(1), pp.59–64. Doi: 10.1021/i160057a011

36. Mohammadi, A., Manteghian, M., Haghtalab, A., Mohammadi, A.H., and Rahmati-Abkenar, M., 2014. Kinetic study of carbon dioxide hydrate formation in presence of silver nanoparticles and SDS. *Chemical Engineering Journal*, 237, pp.387–395. Doi: 10.1016/j.cej.2013.09.026

Persian Abstract

چکیده

یکی از روش‌های جذب گاز گلخانه‌ای کربن دی اکسید، تشکیل هیدرات است. در کار حاضر سینتیک تغییرات حجم آب واکنش نداده، هیدرات کربن دی اکسید تشکیل شده و همچنین گاز واکنش نداده داخل رآکتور با گذشت زمان بررسی شد. آزمایش‌ها در یک رآکتور بدون همزن دوجداره به حجم ۱۶۹ سانتیمتر مکعب و در دمای ۲۷۵/۱۵ کلوین و فشار ۳ مگاپاسکال و با روش حجم ثابت – دماثابت انجام شد. نتایج آزمایش‌های انجام شده نشان داد با گذشت زمان حجم آب واکنش نداده کاهش یافت و حجم هیدرات تشکیل‌شده افزایش یافت. با در نظر گرفتن متفاوت بودن حجم مولی هیدرات تشکیل شده و حجم مولی آب واکنش داده در شرایط آزمایش، تغییرات حجم گاز داخل رآکتور با گذشت زمان محاسبه شد. حجم گاز داخل رآکتور از ۱۴۴ سانتیمتر مکعب در ابتدای فرآیند به ۱۴۱/۶۲ سانتیمتر مکعب در انتهای واکنش کاهش یافت. با کاهش فشار در طول فرآیند تشکیل هیدرات دی اکسید کربن، مقدار عدد هیدرات از ۶/۰۴۷ mol/mol به ۶/۱۰۹ mol/mol افزایش یافت.